



Deposited via The University of Leeds.

White Rose Research Online URL for this paper:

<https://eprints.whiterose.ac.uk/id/eprint/118153/>

Version: Accepted Version

Article:

Agbro, E and Tomlin, AS (2017) Low Temperature Oxidation of n-Butanol: Key Uncertainties and Constraints in Kinetics. *Fuel*, 207. pp. 776-789. ISSN: 0016-2361

<https://doi.org/10.1016/j.fuel.2017.06.086>

(c) 2017, Elsevier Ltd. This manuscript version is made available under the CC BY-NC-ND 4.0 license <http://creativecommons.org/licenses/by-nc-nd/4.0/>

Reuse

Items deposited in White Rose Research Online are protected by copyright, with all rights reserved unless indicated otherwise. They may be downloaded and/or printed for private study, or other acts as permitted by national copyright laws. The publisher or other rights holders may allow further reproduction and re-use of the full text version. This is indicated by the licence information on the White Rose Research Online record for the item.

Takedown

If you consider content in White Rose Research Online to be in breach of UK law, please notify us by emailing eprints@whiterose.ac.uk including the URL of the record and the reason for the withdrawal request.

Low Temperature Oxidation of *n*-Butanol: Key Uncertainties and Constraints in Kinetics
Edirin Agbro¹, Alison S. Tomlin¹

¹School of Chemical and Process Engineering, University of Leeds, Leeds, LS2 9JT, United Kingdom.

*Corresponding author: A.S.Tomlin@leeds.ac.uk

Abstract

A recent chemical kinetic mechanism (Sarathy et al., 2012) describing the low temperature oxidation of *n*-butanol was investigated using both local and global uncertainty and sensitivity methods within the context of predicting ignition delay times in a rapid compression machine ($T = 678\text{--}898\text{ K}$, $\phi = 0.5\text{--}2.0$, $P = 15\text{ bar}$) and species profiles in a jet stirred reactor ($T = 800\text{--}1150\text{ K}$, $\phi = 0.5\text{--}2.0$, $P = 10\text{ atm}$) in order to determine the most important reactions driving the predictive uncertainty, and the constraints provided by the experimental measurements. A global sampling technique was employed for the determination of predictive uncertainties, and a high dimensional model representation (HDMR) method was further utilized for the calculation of global sensitivity indices following the application of a linear screening method. The calculated global sensitivity indices were used to identify and rank the rate parameters driving the predicted uncertainties across the conditions studied. Predicted ignition delay distributions spanning up to an order of magnitude indicate the need for better quantification of the most dominant reaction rate parameters. The calculated first-order sensitivities from the HDMR study show the main fuel hydrogen abstraction pathways via OH as the major contributors to the predicted uncertainties. Sensitivities indicate that no individual rate constant dominates uncertainties under any of the conditions studied, and that the target outputs are largely insensitive to the total rate of OH with *n*-C₄H₉OH. However, strong constraints on the branching ratio for H abstraction by OH at the α and γ sites are provided by the RCM measurements. In the JSR simulations, predicted *n*-C₄H₉OH and CH₂O concentration profiles at $T = 800\text{ K}$, were particularly sensitive to H abstraction reaction by HO₂ from the α site. Although abstraction by OH from the α site plays an important role for predicted *n*-C₄H₉OH profiles at higher temperatures, in general, better constraint is provided on the *n*-C₄H₉OH + HO₂ abstraction rate by the measured concentration profiles of *n*-C₄H₉OH and CH₂O at lower temperatures than for abstraction by OH.

Keywords: *n*-butanol; ignition delays; rapid compression machine; global sensitivity; uncertainty quantification

1.0 Introduction

Due to the need to address issues related to climate change, there is interest in seeking fuels which may be generated from renewable sources including from biomass [1]. Alcohols such as methanol, ethanol and butanol are being projected as satisfactory fuels that could be produced from renewable sources, and used successfully within internal combustion engines. Alcohols, along with other oxygenated fuels, have been shown to have the potential to improve engine performance and emissions because of some of their unique physical and chemical properties [2-4]. There is presently some support for bio-butanol as a potential replacement for ethanol in spark ignition (SI) and compression ignition (CI) engines due to several advantages. Its higher heating value combined with higher stoichiometric air-fuel ratio, allow higher blending levels of butanol in gasoline than can be achieved for ethanol without changing regulations, engine control systems, and distribution networks. Moreover, butanol has a lower latent heat of vaporization than ethanol reducing issues with fuel atomization and combustion during cold start [5]. It is less corrosive and less prone to water absorption than ethanol, allowing it to be transported using existing fuel pipelines. It also has a higher cetane number than ethanol, lower vapour pressure, similar viscosity to diesel and improved miscibility in diesel [6].

Experimental testing of bio-butanol in SI and CI engines has shown promise. However, a detailed investigation and understanding of the behaviour of this new fuel in real engines can be greatly assisted through modelling [7-9], particularly to improve our understanding of the key kinetic processes that drive combustion over a range of temperatures and pressures. In order to accurately reproduce the combustion and emission characteristics of the target fuel during the simulation of SI and CI engines, accurate and reliable detailed chemical kinetic models of fuel oxidation are needed. While the combustion chemistry of common hydrocarbon fuels such as ethanol and dimethyl ether are qualitatively relatively well understood, chemical kinetic modelling studies of the larger alcohols like the butanol isomers at temperature and pressure conditions of relevance to the engine are limited [10-12].

A number of recent studies addressing the chemical kinetic modelling of bio-butanol combustion have been performed [13-19]. Most of the mechanisms developed to date focus on high temperature ($T > 1000$ K) reaction classes and have not been specifically designed for application to the prediction of ignition behaviour at lower temperatures. However recently, Sarathy et al. [12] proposed a detailed reaction mechanism that includes both low and high

temperature reaction pathways for the four isomers of butanol, with reaction rate parameters determined from experimental data, *ab initio* studies and estimations based on bond dissociation energies. For certain key reactions, modifications to rate constants were made (within parameter uncertainties) as part of the validation study of [12], in order to improve agreement with experimental data.

The current work is fundamentally driven by the search for a suitable describing *n*-butanol oxidation for subsequent simulations of *n*-butanol combustion in CI and SI engines. The detailed chemical kinetic scheme of *n*-butanol proposed by Sarathy et al. [12] is investigated in both a rapid compression machine (RCM) and a jet stirred reactor (JSR) with ignition delays and concentrations profiles of key species respectively forming the set of predictive targets. The predictive capability of the Sarathy mechanism, in terms of its ability to accurately reproduce the low temperature properties (auto-ignition and species concentrations) of *n*-butanol is investigated by comparing predicted data from simulations with measured experimental data over a temperature range of $T = 678\text{-}898$ K, an equivalence ratio range of $\phi = 0.5\text{-}2.0$, at pressures of 15 and 30 bar.

Kinetic models of complicated fuels are usually made up of a large set of elementary reactions which are quantitatively described by rate parameters and thermodynamic and transport data for the species. A large number of the rate parameters are, by necessity, determined using semi-empirical estimation approaches (e.g. group additivity methods) because of the difficulties associated with the experimental measurement of such large numbers of rate parameters. This however has the disadvantage of potentially introducing large uncertainties in the determined parameter values and therefore the model as a whole [20]. As a result, even if validated against a range of target experimental data sets using more fundamental combustion apparatuses (such as RCMs, JSRs, premixed and diffusion flames etc.), a model could easily fail when utilised under practical engine conditions that are outside the range in which it is validated or constrained.

Although local sensitivity methods have been applied to the butanol scheme in previous modelling work [12, 21] for importance ranking of key reactions, it does not however account for the impact of the inherent uncertainties in the input rate parameters on the predictive uncertainties. On the other hand, global uncertainty and sensitivity methods provide an understanding of the predictive output uncertainties as well as details on their main

contributing parameters, even where the relationships between the input parameters and predicted target output are highly nonlinear [20]. In addition, since they are based on estimating the contribution of uncertainties to predictive variance, selecting particular experimental observations as predictive targets allows the use of global sensitivities in exploring the extent to which a particular observable can constrain key parameters. Therefore, the sensitivity of predicted ignition delays within an RCM and species concentrations in a JSR to possible uncertainties within the input data of the kinetic scheme (in this case, rate parameters) is investigated here via global uncertainty and sensitivity analyses in order to evaluate the constraints provided by different experimental set-ups on the key reaction rate parameters i.e. to what extent experimental observables can help to narrow the range of uncertainty for the sensitive input parameters.

2.0 Methodology

The Sarathy *n*-butanol mechanism was used as the basis for the simulations of both RCM ignition delays and species profiles within a JSR. A local sensitivity analysis was first used to screen for important reactions for the conditions studied and a selected group of key reactions was then used within the global analysis. For the global uncertainty analysis, a global sampling method was used to vary parameters within uncertainty limits proposed in the study based on available data for each reaction. Variance based methods were then used to propose uncertainties for predicted targets and these were compared with measured data from the literature. Global sensitivity methods were subsequently used to identify the main reactions contributing to the predicted output variance and therefore to explore the chemical pathways driving the observed responses.

2.1 Ignition delay modelling in RCMs

The Cantera software libraries (version 2.1.1) [22] were used within the Python environment to numerically model the *n*-butanol fuelled RCM in line with the experimental conditions and data given by Weber et al. [23] and recent data obtained from the RCM in Leeds. The RCM used by Weber et al. has been described in detail in [24]. In the experimental setup [23], *n*-butanol/O₂/N₂ mixtures were investigated over a compressed temperature range of 679-925 K, compressed pressures of 15 and 30 bar, at ϕ 's of 0.5, 1.0 and 2.0. The modelling approach adopted here is in line with that of Weber et al. [23], in which both compression and post compression events are accounted for. Volume traces which inherently account for the heat losses during both compression and post compression effects were used as input into the auto-

ignition simulations. According to [23], the volume traces for the full event were determined from the measured pressure trace of the non-reactive experiment using the isentropic core relations and temperature-dependent mixture specific heat ratios. The volume profiles were implemented during each time step using a python-based subroutine obtained from the GitHub account of Weber [25] alongside an in-house Cantera based RCM code. The volume traces used in this study are available from [26].

2.2 Definition of ignition delay

The computed ignition delay time is defined as the time from the end of compression (at top dead centre, TDC) to the point of maximum rate of pressure rise $\left(\max\left(\frac{dP}{dt}\right)\right)$.

Appropriate tolerance criteria were chosen to ensure sufficiently stable and well converged solutions for the chosen kinetic scheme.

2.3 Species concentration modelling in the JSR

The modelling of the JSR was also performed within the Python environment using a Cantera set of libraries according to the experimental specification of Dagaut et al. [14] at $P = 10$ atm, $T = 800$ - 1150 K and $\phi = 0.5$ - 2.0 . The JSR set up fully described in [14], is comprised of a 4 cm diameter sphere constructed from fused silica to reduce the effect of wall catalytic reactions and supplied with four 1 mm internal diameter nozzles which helps to admit the gases and at the same time facilitate the mixing of the gases with the reactants. The JSR was chosen for the study because of its relevance in fundamental kinetics and its capacity for investigating fuel effects within the low temperature and intermediate temperature regime. The aim was to determine whether it provided a different set of constraints on the mechanism when compared to low temperature ignition delays. Moreover, the simplicity of the JSR model, which typically, makes it possible to attain high levels of homogeneity in the reactor during the steady state experiments, makes it computationally feasible when coupled with global sampling techniques even when the sample size required is in the order of many thousands.

For the sensitivity analysis of the JSR simulations, a constant residence time of 1.7 s was employed at a constant pressure of 10 atm, and $\phi = 1$ with an initial temperature of 800 K which was increased stepwise by 30 K. A time step of 0.2 s was utilised alongside appropriate tolerance limits in order to attain convergence to steady state. In the context of uncertainty

and global sensitivity analysis, only the predicted steady state mole fractions of species carbon monoxide (CO) and formaldehyde (CH₂O) are considered for further investigation because of their key role as pollutants along with the parent fuel *n*-C₄H₉OH.

2.4 Chemical kinetic model

The mechanism adopted is the recent butanol mechanism, proposed in [12]. The kinetic model, containing 426 species and 2335 mainly reversible reactions, was constructed based on the 1-butanol kinetic scheme of [16] by upgrading the mechanism with the primary reactions of tert-butanol, 2-butanol, and iso-butanol and related radical reactions.

Calculations of rate coefficients for pressure dependent reactions were achieved within Cantera using both the Troe formulation [22] and interpolation based on the PLOG approach depending on the requirements of the scheme. Using the PLOG approach, Arrhenius expressions are given at particular pressures and logarithmic interpolation is used for pressures in between [22].

2.5 Screening approach

Since only a few key reactions are likely to greatly influence the accuracy of the predicted targets, computational time can be saved if these reactions are identified for inclusion in global sensitivity analysis, whilst parameters of low sensitivity are retained at their nominal values. This allows for smaller sample sizes to be used without compromising the sparsity of the input space. A screening approach based on the brute force local sensitivity method was therefore performed for a range of conditions in [23] to identify the key reactions that influence the ignition delay at compressed (TDC) conditions of 15 bar, $T = 678\text{-}898$ K and $\phi = 0.5\text{-}2.0$ and the predicted species concentration profiles at a pressure of 10 atm, for $T = 800\text{-}1150$ K and $\phi = 0.5\text{-}2.0$. The sensitivity of the target output to each reaction in the kinetic model was calculated based on 30 % increase of the reaction rates from their nominal value. Normalised changes to the target quantity were then calculated and based on a threshold of sensitivity coefficient $S_i > 2\%$, a total of 40 reactions were screened for the RCM study and 50 for the JSR. Both set of reactions were then taken forward for further analysis by global uncertainty and sensitivity methods. The set of screened reactions and their normalised local sensitivity indices for selected conditions are presented in section 3.2.

2.6 Global uncertainty and sensitivity analysis

In the global approach, the uncertainty in the selected input parameters is propagated through the model using global sampling in order to provide distributions and therefore uncertainties on the predicted ignition delays and species concentrations. Global sensitivity analysis is then performed in order to rank the contribution of each parameter to the overall output uncertainty, represented by the output sample variance. The global sensitivity method allows one to be able to investigate the impact of model input parameters (e.g. reaction rates) across their entire uncertainty range and also to account for the effect of parameter interactions.

Prior to performing global uncertainty and sensitivity analysis, uncertainty factors (G_i) were assigned to each of the screened reactions based on values evaluated in the reviews of reviews of Baulch [27-29] and Tsang and co-workers [30, 31] where available. For reactions without evaluated uncertainties, data available on National Institute of Standard and Technology (NIST) website representing several studies was employed to estimate the uncertainty of the input parameter. In situations where there were no evaluations and sufficient studies within NIST (experimental or theoretical) to determine the uncertainty of in the rate of a specific reaction from the spread of data, an uncertainty factor of 2 was chosen for the sensitivity calculations. An uncertainty factor of 2 was specifically chosen for the RCM study as higher uncertainties resulted in situations where the model did not produce an ignition event or would produce ignition during compression. A factor of 2 may be optimistic for reactions with rates determined by theory, group additivity or estimation, but the results will show that it already leads to quite large uncertainties within the predictive targets.

The global technique employed here is built around a sampling approach in which many simulations are carried out with samples covering the entire domain of the defined input space. A low discrepancy sampling sequence (Sobol's quasi-random sequence) is employed because of its ability to converge faster (in terms of output mean and variance) compared to standard Monte Carlo random sampling. The Sobol' sequence represents a set of quasi-random numbers between 0 and 1 generated for each of the selected input parameters across the chosen sample size N . This sequence is then used to create a sample of rate parameters within the uncertainty range ($k_i/G_i, G_i \times k_i$) which is uniform in the space of $\log(k_i)$, where k_i is the original rate parameter in the scheme, k_i/G_i is the lower limit and $G_i \times k_i$ is the upper limit. The log rate constants within the chosen uncertainty range are uniformly distributed, as they have been assumed to have equal probability of being the actual rate parameter value. This

approach is fairly typical for schemes with estimated parameters since insufficient information is available to take a probabilistic approach.

Following the sampling and performance of model runs, there is a need to estimate the global sensitivity index - a factor that gives an indication of the importance ranking of input parameters that contribute most to the variance in the predicted output. Surface response methods (SRMs), are commonly employed to investigate the relationship between the input and output distributions [32, 33]. In the SRM method based on high dimensional model representations (HDMR) employed here, the sensitivity indices are calculated using a functional meta-model fitted to sample input-output distributions that is based on the quasi-random sample (QRS) of full model runs. The accuracy of the calculated sensitivities is dependent on the accuracy of the constructed meta-model which in turn is a function of the sample size, the fitting approach used in constructing the meta-model and the complexity of the surface response [32]. A total sample size of $N = 256$ was used for the uncertainty study (in order to estimate uncertainties on predicted targets) while a sample size N ranging from 2048-4096 was used for the QRS-HDMR study in order to obtain accurate HDMR meta-model fits based on up to 10th order orthonormal polynomials and a coefficient of determination $R^2 > 90\%$ for ignition delay predictions. A full description of the QRS-HDMR method can be found in [34].

3.0 Results and Discussion

3.1 Comparison of model predictions with experimental data

3.1.1 RCM studies

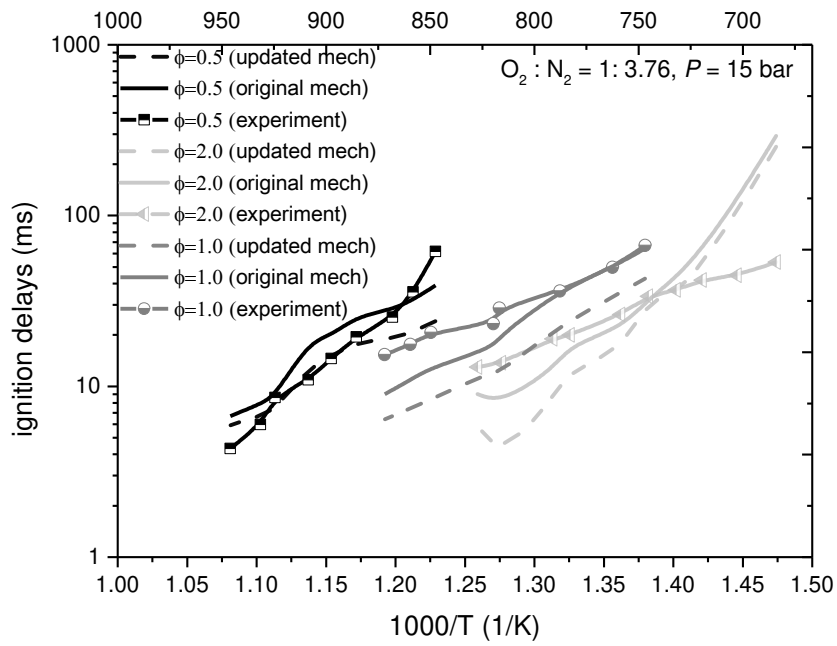


Fig. 1: Comparison of ignition delays predicted by Sarathy model with Weber et al. data [23] for conditions of $P = 15$ bar and $\phi = 0.5$ and 2.0

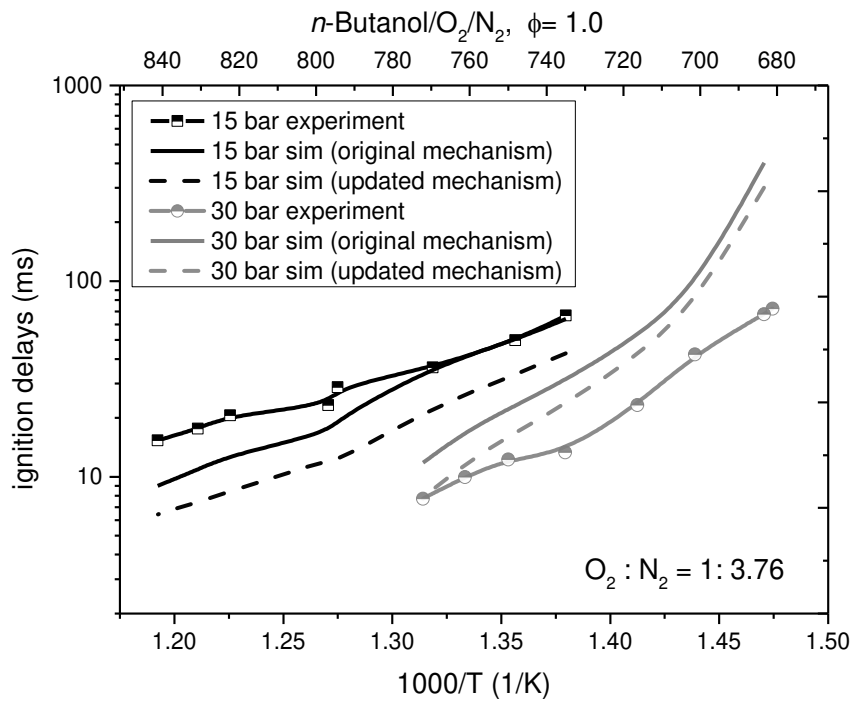


Fig. 2: Comparison of ignition delays predicted by Sarathy model [12] with Weber et al. data [23] under stoichiometric conditions at 15 bar and 30 bar

Figure 1 shows a comparison of predicted ignition delays with the data from Weber et al. for a compressed pressure of 15 bar, $T = 678 - 925$ K and $\phi = 0.5 - 2.0$. In common with Sarathy et al. and Weber et al. [12, 23], we find that the RCM data is predicted to a reasonable level of accuracy across the entire equivalence ratio range. However, under rich conditions, the model's over-prediction of the ignition delay data could be over a factor of 5 for the low temperature region (i.e. $T < 700$ K). Under stoichiometric conditions, at a higher pressure of 30 bar (Fig. 2), which is above the pressure range at which the model was constrained by ignition delays, the model over-predicts the Weber data by a factor of about 2 across a major part of the temperature range. In addition, the decrease in ignition delays when pressure is increased from 15 to 30 bar is under-represented by the model. It is also apparent from Figs. 1 and 2 that *n*-butanol does not exhibit the well-known two-stage, NTC behaviour commonly seen for linear alkanes and shown for DME ignition delays in our previous work [34].

3.1.2 Jet stirred reactor (JSR) studies

Figure 3 reveals how the experimental species mole fractions measured in the JSR compare with the predicted species profiles using the mechanism of Sarathy [12] at $\phi = 1$ and $P = 10$ atm. Similar to reported in [14], we see that the predicted species concentrations of CO and CH₂O are in very good agreement with the measured profiles across a major part of the temperature range except for temperatures below 830 K where the model significantly over-predicts the experimental values up to a factor of 9 for CO and 8 for CH₂O. *n*-butanol species profiles were predicted reasonably well in the temperature range 800 - 920 K but not at higher temperatures (above 920 K) where the model displayed higher levels of reactivity compared to the measured data. In general, the model prediction of the peak point for the three species considered in the study is very good. The possible causes of the discrepancies between the simulations and experimental data will be discussed further in the subsequent sections.

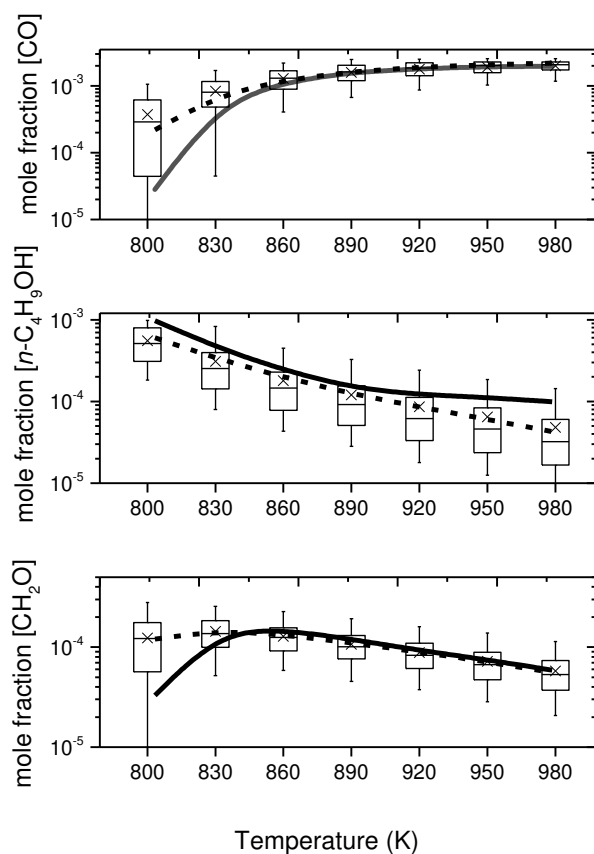


Fig. 3: Comparison between experimentally measured species profiles (solid line) and simulated profiles using the nominal parameter values (dashed line). The boxes represent 25th and 75th percentiles while whiskers represent 5th and 95th percentiles respectively based on a quasi-random sample of 256 model runs. The large crosses and line in the middle of box represent the mean and median of predicted output from the 256 simulations respectively

3.2 Local sensitivity analysis

3.2.1 RCM analysis

Local sensitivity analysis employing the brute force method was performed within the framework of ignition delay prediction in the n -butanol fuelled RCM for a range of conditions across $T = 678 - 898$ K, $\phi = 0.5 - 2.0$ and $P = 15$ bar. The results are illustrated in Fig. 4 for 15 of the most sensitive reactions at $T = 725$ K, $\phi = 1$ and $P = 15$ bar. The results show that the most sensitive reactions at low to intermediate temperatures are the branching fractions of the main fuel H abstraction reactions via OH with the abstraction from the α -carbon site playing the most dominant role in agreement with the low temperature analysis in [12, 35].

The α -hydroxybutyl radical formed via hydrogen abstraction from the α site reacts very quickly with oxygen to produce butanal ($n\text{-C}_3\text{H}_7\text{CHO}$). This reaction route which has a similar sensitivity to the OH abstraction route from the γ site, is similar to the termination (inhibiting) step in the low temperature oxidation of alkanes leading to the formation of alkenes and HO_2 radicals that compete with the isomerisation and chain branching reactions by direct elimination from RO_2 . As reported in [12], the current rate parameterisation of this reaction ($1\text{-hydroxybutyl} + \text{O}_2 = n\text{-C}_3\text{H}_7\text{CHO} + \text{HO}_2$) is based on the theoretical evaluation of Silva and Bozzelli [36] and is majorly responsible for the very slow reactivity exhibited by the model across the low temperature range (Figs. 1 and 2) especially under rich conditions and at high pressure. Figure 5 shows the plot of the normalised local sensitivities for 20 of the most dominant reactions at $T = 814\text{ K}$, $P = 15\text{ bar}$ and $\phi = 0.5$ alongside the sensitivities of the same reactions at $T = 898\text{ K}$. Figure 5 clearly indicates that as temperature is increased, the reactions of $n\text{-C}_4\text{H}_9\text{OH} + \text{HO}_2$ and H_2O_2 become more important in terms of the accurate prediction of auto-ignition in the high temperature region. This is in agreement with the local sensitivity result of [35] where the fuel specific reaction of $n\text{-C}_4\text{H}_9\text{OH} + \text{HO}_2 = \text{H}_2\text{O}_2 + \text{C}_4\text{H}_8\text{OH-1}$ and $\text{H}_2\text{O}_2 = 2\text{OH}$ were both identified as the reactions with the most influence on ignition delays at higher temperatures (above 1000 K).

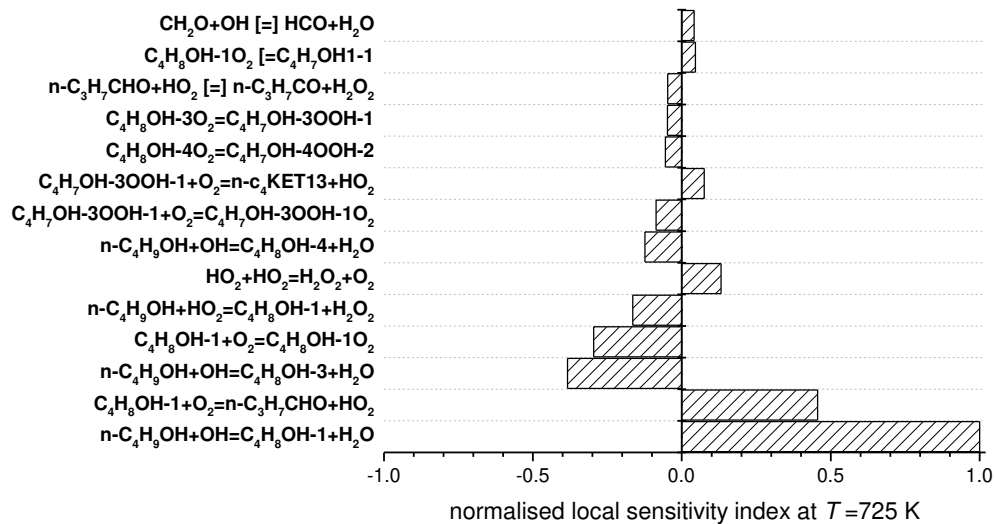


Fig. 4: Normalised local sensitivity analysis for predicted log (ignition delay) of n -butanol/air mixtures at $P = 15\text{ bar}$, $T = 725\text{ K}$ and $\phi=1$

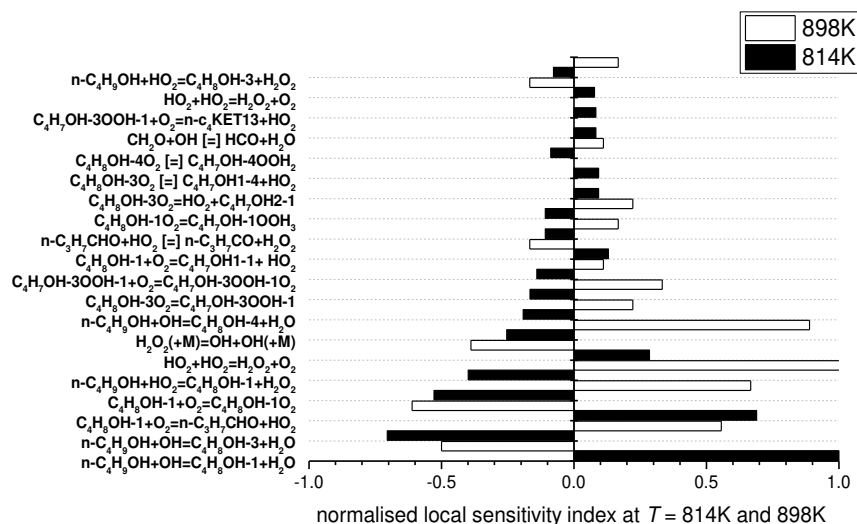


Fig. 5: Result of local sensitivity analysis for predicted log (ignition delay) of *n*-butanol/air mixtures at $P = 15$ bar, $T = 814$ K and 898 K and $\phi = 0.5$

3.2.2 JSR analysis

Figure 6 shows the normalised local sensitivity indices for the first 20 most important reactions influencing the predicted concentration profiles of *n*-C₄H₉OH, CH₂O and CO at 830 K. While the high temperature decomposition reaction of H₂O₂ (H₂O₂ (+M) = OH +OH) is found to dominate the predicted concentration profiles of the three chosen species at 830 K, H abstraction reactions from the α and γ sites of *n*-C₄H₉OH alongside reactions involving HO₂, ($n\text{-C}_4\text{H}_9\text{OH} + \text{HO}_2 = \text{C}_4\text{H}_8\text{OH-1} + \text{H}_2\text{O}_2$, $\text{HO}_2 + \text{HO}_2 = \text{H}_2\text{O}_2 + \text{O}_2$) are also found here to play key roles in the prediction of *n*-C₄H₉OH and CO. Interestingly, the H abstraction reactions, particularly the ones from the α -carbon site are also the ones that dominated the predicted ignition delay times within the RCM. In terms of the predicted formaldehyde concentrations, the H abstraction reactions from the γ and δ site alongside reactions involving CH₂O and HO₂ are among the most important reactions at 830 K.

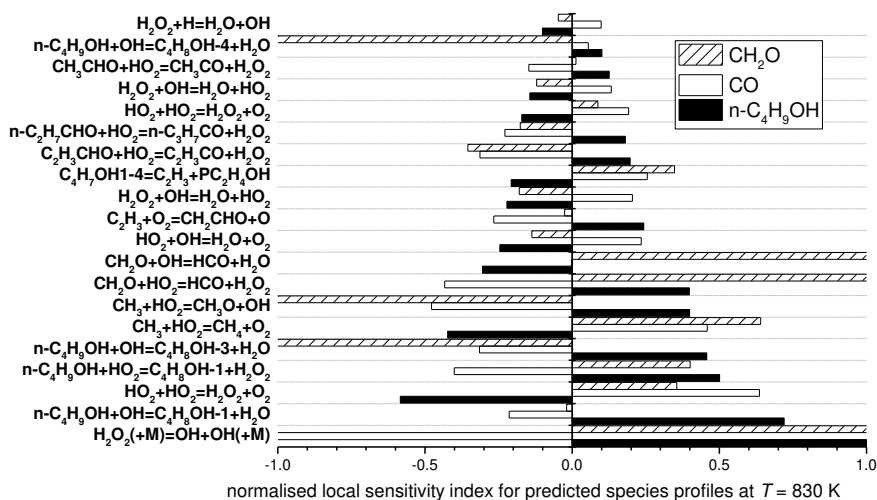


Fig. 6: Result of local sensitivity analysis for predicted species profiles of *n*-butanol/air mixtures at $P = 10$ bar, $T = 830$ K and $\phi = 1$

3.3 Uncertainty study

3.3.1 RCM analysis

Figure 7 shows the predicted ignition delay distributions based on the propagated uncertainties in the model for the case of $\phi = 1$, at $P = 15$ bar, and $T = 725 - 839$ K. Although the original model appears to predict the ignition delay data quite well at lower temperatures, with the experimental values close to the median of the predicted distribution, uncertainties in the predicted ignition delays are quite large in this region; up to at least plus or minus one order of magnitude. At higher temperatures, the agreement at nominal parameter values is less good, although the predicted uncertainty distributions are much smaller (up to about 50% less) and the experimental values lie close to the mean predictions. Overall, within the suggested uncertainties for the model, there is agreement with the experiments across the temperature range. The large uncertainties in predicted delays especially at the lower temperature region do however, indicate the need for a more accurate knowledge of the dominant rate parameters in the scheme if the scheme were to be reliably utilised for auto-ignition predictions under real engine conditions. Particular focus should be paid to temperature dependencies of the rate parameters. Via a global sensitivity study we can determine which parameters contribute most to these predictive uncertainties. Secondly we can determine how the experimental measurements constrain these parameters under the different conditions studied.

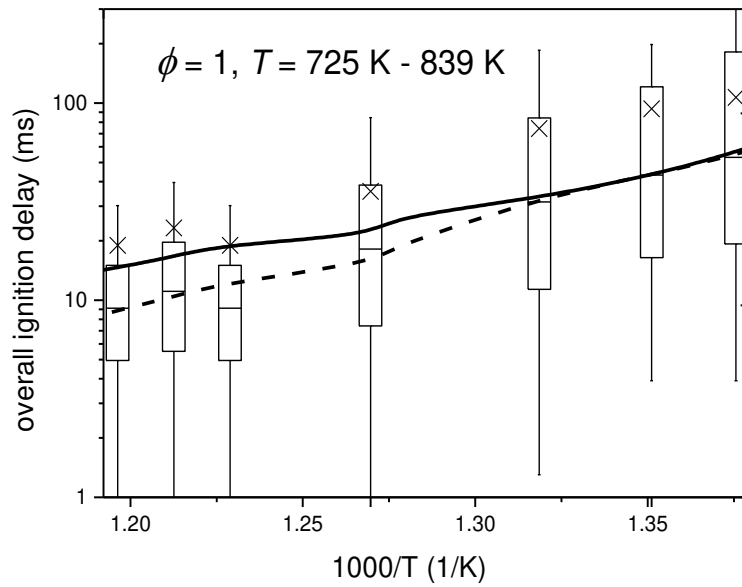


Fig. 7: Comparison of predicted *n*-butanol ignition delays using nominal values (dashed line) with experimental data (solid line) from [23]. Boxes represent 25th and 75th percentiles while whiskers represent 5th and 95th. The large crosses and line in the middle of box represent the mean and median of predicted output from the 256 simulations respectively

The differences in the location of the mean and median of the predicted output also reveal that the data represents a non-Gaussian distribution. Figure 8 shows a typical distribution of the predicted log ignition delays at $T = 787$ K and $\phi = 1$ for the 256 runs from the quasi-random sample. The data is skewed to the left with a tail and conforms more to a lognormal distribution rather than a normal distribution. This means that in a low number of samples very short ignition delays are predicted leading to the whiskers and outliers of the data set shown in Fig. 7. Such tails are often an indication of interactions between parameters driving large variability in the predicted targets. On the face of it, the predicted output uncertainties shown in Fig. 7 seem large, particularly since they are based on input uncertainties of no greater than a factor of 2 (see supplementary material) in many cases. The reason is that within the sampling we are allowing each rate parameter to vary across its whole range without assuming any correlations between input data. The prediction of ignition delays is strongly influenced by the relative rates that lead to chain branching compared to those that lead to chain propagation or termination. Therefore the relative rates of the H abstraction from the fuel at different sites are likely to be influential and if competing reaction channels are allowed to vary across their whole range, tails in the predicted distribution of target outputs such as ignition delays may result from the pairing of extreme values of the input parameters for the competing channels. This point will be further discussed following the presentation of the global sensitivity indices in the next section.

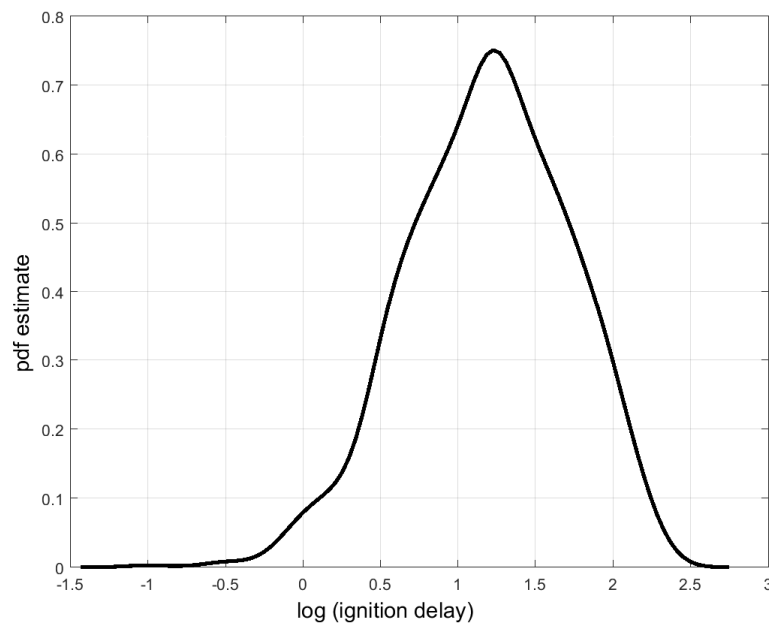


Fig 8: Typical distribution of predicted log (ignition delay (ms)) at $T = 787$ K and $\phi = 1$

3.3.2 JSR analysis

Figure 3 also presented the predicted distribution of the concentration profiles of CO, CH₂O and *n*-C₄H₉OH from the JSR study, while incorporating the uncertainties of the most dominant input parameters in the simulations, superimposed on the predicted single profiles of the same species. Figure 3 shows that for CO and CH₂O, the experimental data fall close to the mean of the predicted output distributions except for the lower temperature region ($T < 860\text{K}$) where the experimental data lie within the 25th percentile of the predicted output distributions. For *n*-butanol, the experimental data is close to the 75th percentile for most of the temperature range. In terms of the uncertainty quantification, the predicted uncertainty distributions for CO and CH₂O are quite small at temperatures above 860 K where the model is in good agreement with the measured data but could be up to two orders of magnitude at the lower temperature of 800 K. For *n*-butanol, the predicted uncertainty distributions are largest at the higher temperatures and are within one order of magnitude. In the next section, a global sensitivity approach is employed alongside the HDMR method to identify the key reactions driving the predicted output uncertainties.

3.4 Global sensitivity study

3.4.1 RCM analysis

Figure 9 shows the main first-order sensitivities indices S_i calculated in the HDMR study. The shading for each of the selected reactions is shown on the legend. If all the variance in the predicted output was accounted for by the individual effects of each parameter, then the sum of the S_i would be 1 (equivalent to 100% of the variance). The selected reactions are the seven most important reactions influencing the predicted *n*-butanol ignition delay and account for over 85 % of the variance, highlighting that the uncertainties are dominated by the first-order effects of just a few reactions.

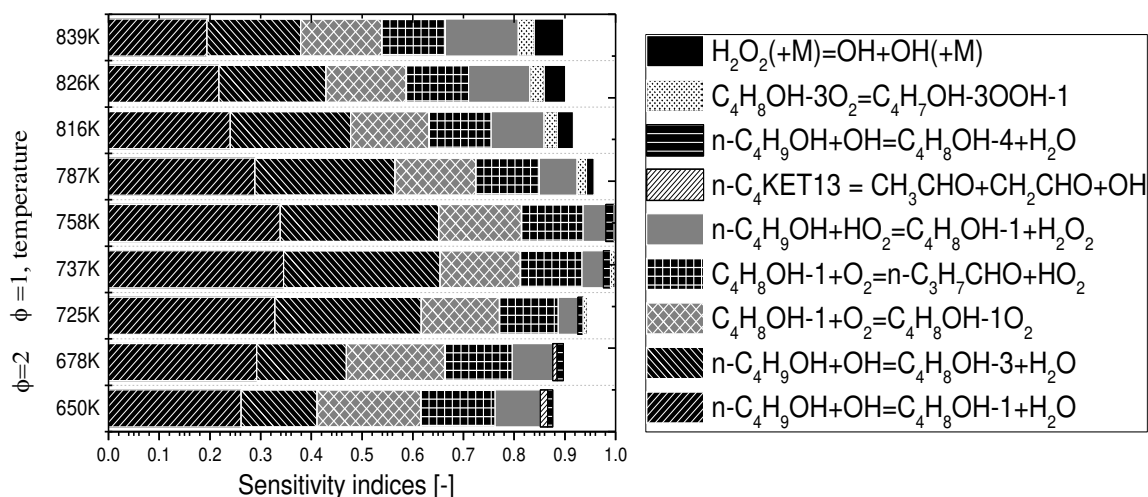


Fig. 9: Main first-order sensitivity indices for simulated log (ignition delay) with respect to reaction rates at selected temperatures, $P = 15$ bar. (Left) Sensitivity indices (Right) legend

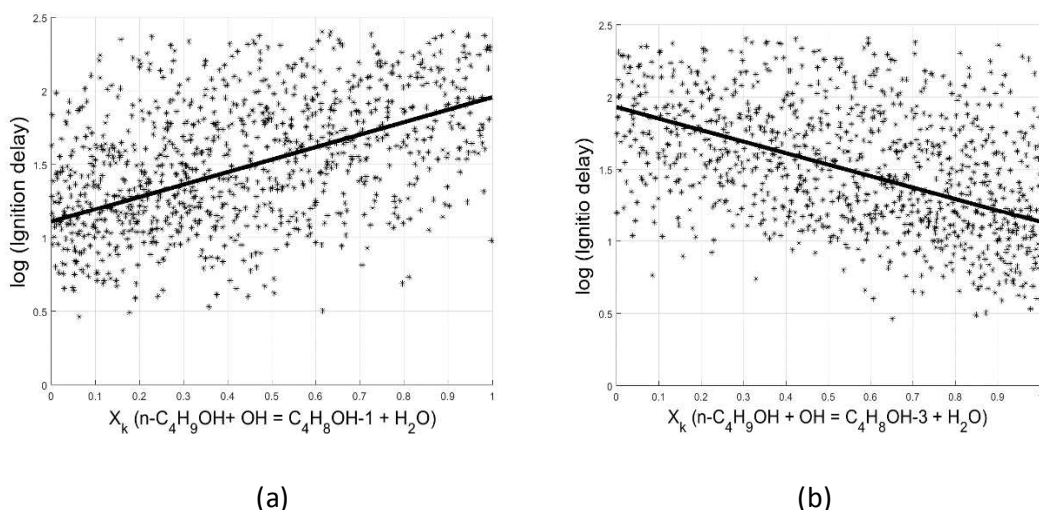


Fig. 10: HDMR component functions (solid line) of simulated log (ignition delay) shown on-top of the scatter for a) $n\text{-C}_4\text{H}_9\text{OH} + \text{OH} = \text{C}_4\text{H}_8\text{OH}-1 + \text{H}_2\text{O}$ b) for $n\text{-C}_4\text{H}_9\text{OH} + \text{OH} = \text{C}_4\text{H}_8\text{OH}-3 + \text{H}_2\text{O}$, $P = 15$ bar, $\phi = 1$, $T = 725$ K

For the stoichiometric conditions studied, the branching fractions of fuel + OH hydrogen abstraction reactions dominate the predicted uncertainties across the entire temperature range (i.e. low-intermediate temperatures). The H atom abstraction reaction from the α site of n -butanol by OH was also identified in a recent paper by Westbrook et al. [37] as being mainly responsible for the octane sensitivity (OS) behaviour of n -butanol. According to [37], the chemical structure of n -butanol in which the OH group is positioned on the first carbon, is a form of electron delocalisation which allows the abstraction from the α -site by OH to be relatively faster. The hydroxybutyl radicals produced as a result of the main fuel oxidation

reactions are consumed via two different type of reaction pathways - one is the oxygen addition reaction (α -hydroxybutyl + O₂) leading to the formation of the peroxy radical (RO₂) that drives auto-ignition, and the other is the termination step that inhibits auto-ignition due to the formation of HO₂. Although it is well known that the isomerisation reaction of the RO₂ dominates auto-ignition chemistry in general low-temperature mechanisms, the dominance of the main fuel hydrogen abstraction reactions is as a result of its key role in determining the amount of fuel that goes to the termination steps compared with how much is available for the chain branching and propagation steps. The contribution from the H abstraction reactions however diminishes with increasing in temperature while contributions from HO₂ chemistry and formation route for H₂O₂ become more significant.

The sensitivities highlight that constraints on the reaction rate coefficients for the H abstraction reactions by OH are better provided by ignition delays at stoichiometric lower temperature conditions since their uncertainties contribute to a larger percentage of the predictive variance. However, no single rate constant dominates, with the two main H abstractions from the α and γ sites showing first-order sensitivities of 0.32 and 0.29 respectively. This means that a wide range of chosen rate constants for these reactions could reproduce the experimental ignition delays with reasonable accuracy. Figure 10 shows the HDMR component functions which highlight the individual response of the predicted targets to changes in the A-factor for these reactions. The data points in these figures represent the individual responses from the quasi random sample whereas the line (component function) illustrates the individual effect of the chosen parameter. If a single parameter dominated uncertainties in the output, then there would be no scatter about the line in such a plot and the sensitivity index for the parameter would be close to 1. In such a case the experimental target could be used to fully constrain the input parameters, or at least to within the accuracy provided by the experimental measurement. However, what we see is a high degree of scatter about the component function, indicating a strong influence from the uncertainties in the other selected input parameters. The measured log ignition delay from experiments under the conditions shown in Fig 10 is just below 1.5. Hence it can be seen that any value of the A-factor can be selected for one of the abstraction rates within its range of uncertainty as long as the other is selected accordingly. Measured ignition delay times therefore offer only weak constraints on the abstraction rates from the individual sites.

Sarathy et al. report [12] discrepancies between the ab initio studies for abstraction from the α site between the studies of Zhou et al. [38] and Zádor et al. [39] and adopted the temperature dependence of [39] to give better agreement with experimental data. H abstraction from the γ site is critical to correctly determining the amount of chain branching which drives low temperature auto-ignition. The rate constant for this reaction was however, subject to large discrepancies between [38] and [39] and hence corrections were made in [12]. The low temperature ignition delays at $\phi = 1$ provide some constraints on this reaction channel ($S_i=0.29$) but there is still a large influence of uncertainties in other key rates (Fig. 10b).

However, if we plot predicted log ignition delay against a scaled ratio of the log reaction rates for these main abstraction reactions from the α and γ sites, leading to $C_4H_8OH-1 + H_2O$ and $C_4H_8OH-3 + H_2O$ respectively, we see an almost linear relationship (Fig. 11), with the scatter resulting from uncertainties in the other main reactions listed in Fig. 9. The sensitivity index for this branching ratio is 0.7 i.e. twice that for the individual rates. On the contrary the sensitivity index for the sum of reaction rates for H abstraction by OH is <0.1 . The analysis therefore demonstrates that ignition delay measurements provide much stronger constraints on the branching ratio than on the overall rate constant for this reaction class; or conversely, that the prediction of ignition delays is largely insensitive to the total reaction rate of *n*-butanol with OH. A recent study by Pang et al. [40] provides rate constant for the overall reaction between *n*-butanol and OH in the higher temperature region (900 -1200 K) but does not present any information on the branching ratios for the different abstraction sites. Although the overall rate constant for OH + *n*-Butanol was measured by Pang to within an accuracy of 20 %, it is important to stress here, that based on the result of the global sensitivity analysis obtained in this study, accurate measurements of the total reaction rate of the parent fuel with OH do not provide sufficient data to accurately determine target outputs such as ignition delays. In addition, there is still scatter in Fig. 11 due to the influence of uncertainties in other channels such as R+O₂. At lower temperatures and richer conditions ($\phi = 2$), where discrepancies between model and experiment were seen in Fig. 1, R+O₂ reactions are equally as important as H abstraction (Fig. 9). The reaction to form butanal+HO₂ is included as a high temperature pathway in [12] but actually shows a higher sensitivity at low temperature rich conditions.

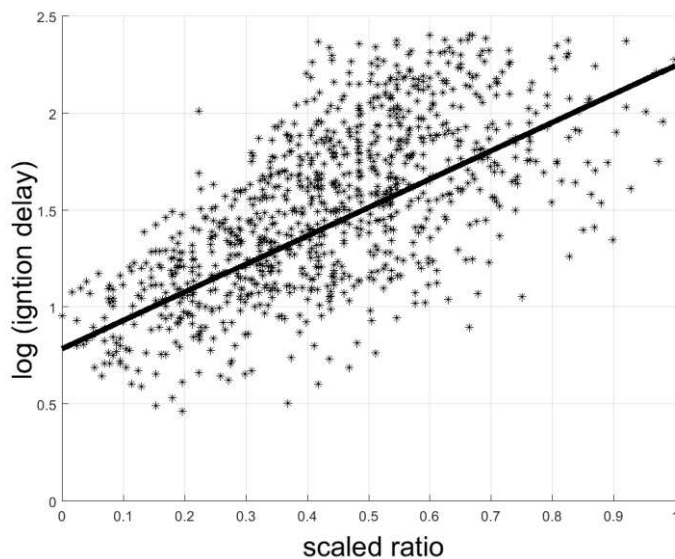


Fig. 11: Scatter plot and HDMR component function for predicted log (ignition delay) against the scaled branching ratio for the two main H abstraction reactions by OH, taking into account uncertainties in the 40 main reactions, $T = 725$ K, $\phi = 1$, $P = 15$ bar

3.4.2 JSR analysis

Figures 12 and 13 show the main global sensitivity indices obtained from the HDMR analysis for the simulated JSR data. Sensitivity coefficients were estimated in the HDMR analysis based on simulations involving 2048 samples. Results shown in Figs. 12 and 13 represent the first-order sensitivity coefficients for the 10 most important reactions influencing the predicted uncertainties for n -C₄H₉OH and CH₂O at two selected temperature points (800 K and 830 K) where the model displayed a very high level of discrepancy in terms of the predicted species profiles. Interestingly, these are also the temperature points that overlap with the temperature conditions studied in the RCM. The selected ten key reactions account for about 55-70% of the overall predicted variance, with the H abstraction reaction by HO₂ leading to formation of C₄H₈OH and H₂O₂ (contributing over 30 %) dominating the uncertainties in both n -C₄H₉OH and CH₂O profiles at 800 K. This same abstraction route for n -C₄H₉OH + HO₂ was found to be the most dominant reaction in [12] in terms of the ignition delay sensitivity at 800 K, and $\phi = 1$ but this was at a much lower pressure of 1 atm. In the HDMR analysis of predicted ignition delay times (Fig. 9), over 85% of the uncertainties were accounted for by only seven reactions, with H abstraction by OH dominating across the temperature range in contrast to n -C₄H₉OH + HO₂ as found in the case of the JSR. Heufer et

al. [35] suggested the use of estimated rate coefficients for *n*-butanol + HO₂ based on alkanes, and this could be the reason for the large discrepancies between the predicted target outputs and measured data. According to Heufer [35], the current parameterisation of this rate is still very poor as variation of the rate coefficients for this same reaction in the mechanisms of Black and Moss [16, 17] can be up to a factor of 20, suggesting the need for more detailed and accurate studies of this reaction across a wide range of temperatures and pressures in order to improve on the level of agreement with experimental data.

As *T* increases to 830 K, the contribution from abstraction by HO₂ diminishes in importance while abstraction reactions by OH become more significant dominated by abstraction from the α site. This sensitivity behaviour is in agreement with the results of local sensitivity analysis carried out in [14] where H-abstraction reactions by OH from the α and γ carbons were captured as the reactions for which *n*-butanol concentrations are most sensitive at high temperatures (*T* = 1050 K). The sensitivities demonstrate as well that H abstraction from the α site is not important at high temperatures for the predicted distribution of CH₂O concentrations, but the reactions of CH₂O + OH and H abstraction from the δ site are significant contributors. It is also clear from the HDMR study that no single reaction dominates the uncertainties at higher temperatures as most of the key reactions are equally significant. A stronger level of constraint is however provided by the measured species profiles of *n*-C₄H₉OH and CH₂O on the *n*-C₄H₉OH + HO₂ abstraction rate at the lower temperature given their estimated sensitivities of 0.34 and 0.35 respectively.

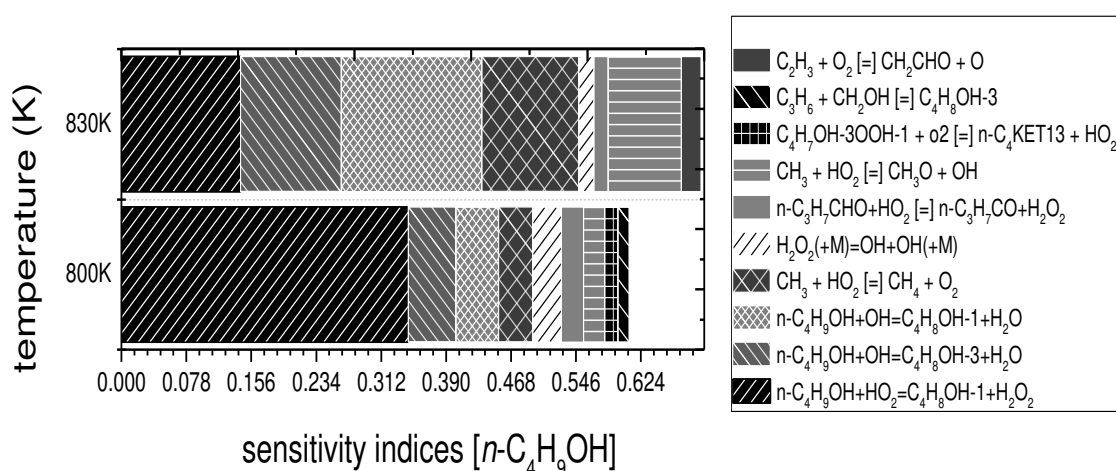


Fig. 12: Main first-order sensitivity indices for simulated n -C₄H₉OH species profiles with respect to reaction rates at selected temperatures and pressure of $P = 10$ atm. (Left) Sensitivity coefficients (Right) legend

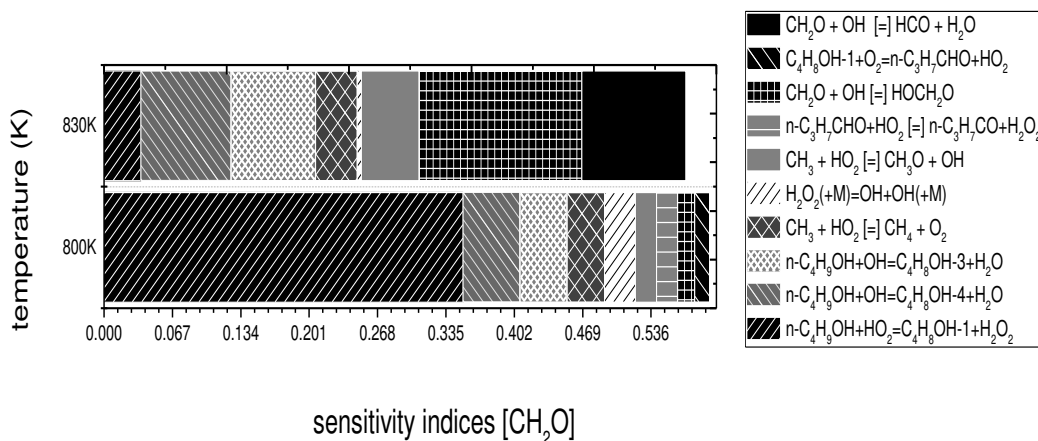
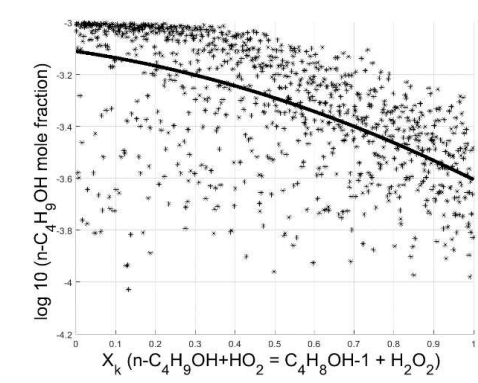


Fig. 13: Main first-order sensitivity indices for simulated CH₂O species profiles with respect to reaction rates at selected temperatures and pressure of $P = 10$ atm. (Left) Sensitivity coefficients (Right) legend

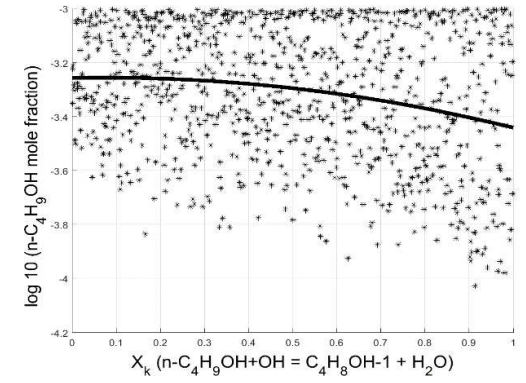
Figure 14 shows the three most important first-order component functions with respect to n -butanol concentrations, and gives an overview of the relationship existing between these input parameters and the predicted output. In each case shown, the middle point on the x-axis (0.5) represents the current nominal value of the A-factor used in the model. Firstly, we can see a nonlinear response to changes in the rate of all three hydrogen abstraction reactions demonstrating the need to compute the model's sensitivities across the entire range of input uncertainties rather than just at the nominal value as seen in local sensitivity analysis. For example in the local sensitivity method employed here prior to the global sensitivity analysis, the reaction of H₂O₂ + (M) = OH + OH + (M) was captured as the most dominant reaction at 800 K across all target species but here in the HDMR analysis (Figs. 12 and 13), the reactions α - n -C₄H₉OH + HO₂, α - n -C₄H₉OH + OH and γ - n -C₄H₉OH + OH are more dominant. From Fig. 14b and Fig. 14c, we can see that the gradients at the nominal input rate for the reactions indicated are less steep (indicating low sensitivity) compared to in the upper part of their input range. The same is true for H₂O₂ + (M) = OH + OH + (M) (Fig. 14d) and this is one reason that local sensitivity indices, computed using the nominal parameter values can be misleading.

Another reason is that the local method does not account for the degree of uncertainty in the parameters and so does not represent the contribution of input uncertainties to the output variance. The response of the predicted *n*-butanol mole fractions to the *n*-butanol abstraction reaction by HO₂ is strongly negative across the entire input uncertainty range (Fig 14a) indicating that a decrease in this rate could potentially lead to better agreement of the model output with measured data but this is still subject to the influence of the uncertainty in the other rate parameters in the system. As the rate of the abstraction reaction by HO₂ is reduced, the impact uncertainties in other reaction rates including the branching fractions of *n*-C₄H₉OH + OH increases, as indicated by the broadening of the scatter.

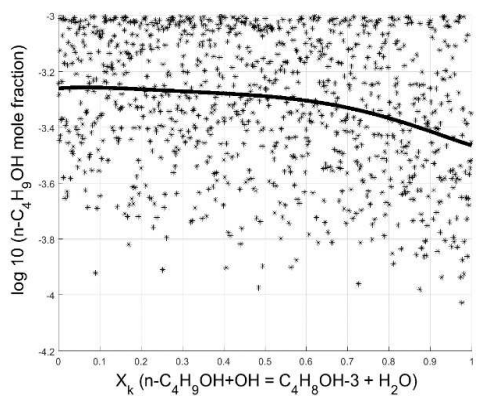
The functional relationship between the abstraction reaction of *n*-C₄H₉OH + OH from the α and γ site (Fig 14b and 14c) shows a strong negative response at the upper part of the input space but the effect saturates at the lower half, indicating that adopting different rate parameters outside the nominal rate for these channels is unlikely to reduce the discrepancy between the model and the measured data. It was shown in section 3.4.1 that ignition delay measurements provide much stronger constraints on the branching ratio than on the overall rate or individual rate constant for this set of abstraction reactions. The first-order sensitivity component functions with respect to formaldehyde mole fractions at 800K are presented in Fig. 15 for the abstraction reaction of *n*-butanol + HO₂ and *n*-butanol + OH abstraction from the γ site. A nonlinear response is also observed in both cases similar to that involving *n*-butanol mole fractions but in this case, the response for *n*-butanol + HO₂ is positive for most of the lower uncertainty range and slightly negative at the upper end. Also, the contribution from the other important parameters to the predicted uncertainty band decreases drastically across the upper part of the input range as indicated by the narrowing of the scatter. For the γ abstraction reaction of *n*-butanol + OH (Fig 15b), a very low gradient is seen at the lower end indicating low sensitivity but the response becomes slightly stronger as we move from the lower part of the input range to the upper part. The experimentally measured log of CH₂O mole fraction is around -4.52 and looking at Fig. 15b, the rate of the abstraction reaction α -*n*-butanol + HO₂ would have to be in the lower part of the input parameter range in order to bring the model's prediction in close agreement with the measured data. This suggests that in this case, the formaldehyde species concentration measurements help to narrow the range of uncertainty for the input parameter i.e. to constrain it further. This was not the case for the *n*-butanol concentration measurements and highlights the utility of measuring important intermediates such as formaldehyde.



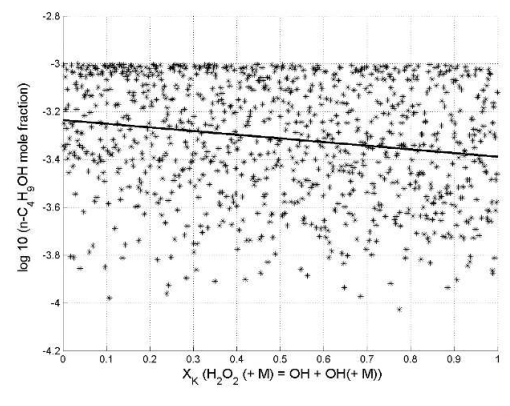
(a)



(b)

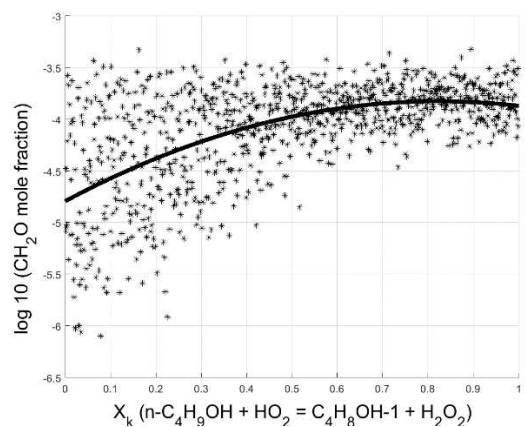


(c)

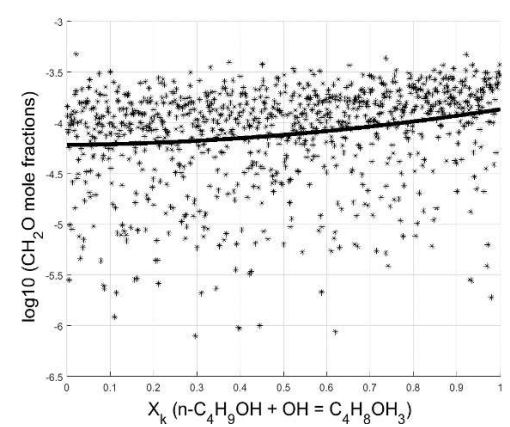


(d)

Fig. 14: First-order component function (solid line) of simulated species profile and scatter at $T = 800\text{K}$, sensitivity of n -butanol to changes in reaction a) $n\text{-C}_4\text{H}_9\text{OH} + \text{HO}_2 = \text{C}_4\text{H}_8\text{OH}-1 + \text{H}_2\text{O}_2$ b) $n\text{-C}_4\text{H}_9\text{OH} + \text{OH} = \text{C}_4\text{H}_8\text{OH}-3 + \text{H}_2\text{O}$ c) $n\text{-C}_4\text{H}_9\text{OH} + \text{OH} = \text{C}_4\text{H}_8\text{OH}-1 + \text{H}_2\text{O}$ d) $\text{H}_2\text{O}_2 + (\text{M}) = \text{OH} + \text{OH} + (\text{M})$



(a)



(b)

Fig. 15: First-order component function (solid line) of simulated species profile and scatter at 800K, sensitivity of CH_2O to changes in reaction a) $n\text{-C}_4\text{H}_9\text{OH} + \text{HO}_2 = \text{C}_4\text{H}_8\text{OH-1} + \text{H}_2\text{O}_2$ b) $n\text{-C}_4\text{H}_9\text{OH} + \text{OH} = \text{C}_4\text{H}_8\text{OH-3} + \text{H}_2\text{O}$

At a higher temperature of 830 K, the prediction of $n\text{-C}_4\text{H}_9\text{OH}$ and CH_2O is relatively less sensitive to the abstraction reaction by HO_2 . At 830 K, n -butanol mole fraction is most sensitive to the abstraction reaction by OH from the γ site (Fig. 16a) while CH_2O mole fraction is driven mainly by the reaction of $\text{CH}_2\text{O} + \text{OH}$ (Fig. 16b). The reaction $\text{CH}_2\text{O} + \text{OH}$ was found to be the most influential reaction contributing about 16 % to the variance in the predicted mole fractions of CH_2O at 830K. Increasing the rate of this reaction (Fig. 16b) could lead to a reduction in the predicted CH_2O mole fractions to give a better match with the experimental data. Another key reaction route on which the accuracy of the predicted CH_2O concentration depends is $\text{CH}_2\text{O} + \text{OH} = \text{HCO} + \text{H}_2\text{O}$ with its uncertainty contributing to over 10% of the variance in predicted CH_2O mole fractions.

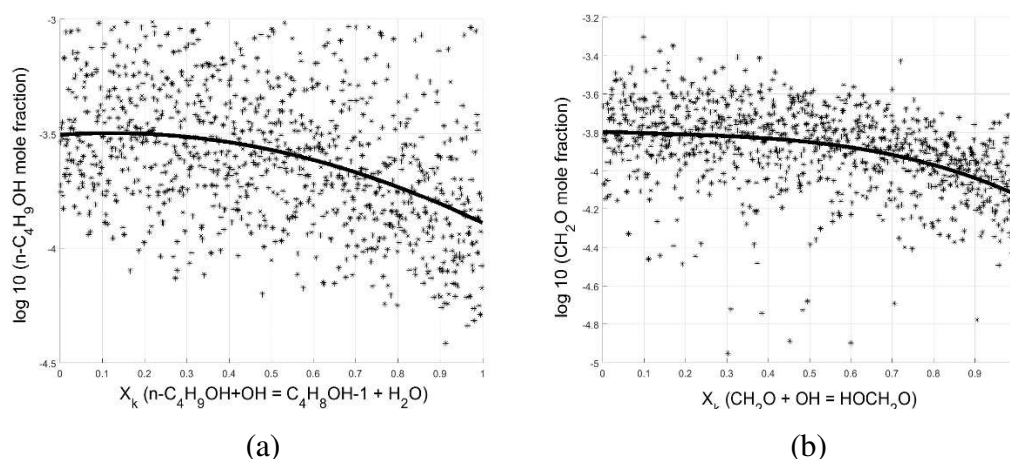


Fig. 16: First-order component function (solid line) of simulated species profile and scatter at 830K, $\phi = 1$. (a) Sensitivity of $n\text{-C}_4\text{H}_9\text{OH}$ to changes in reaction $n\text{-C}_4\text{H}_9\text{OH} + \text{OH} = \text{C}_4\text{H}_8\text{OH-1} + \text{H}_2\text{O}$ (b) Sensitivity of CH_2O to changes in reaction $\text{CH}_2\text{O} + \text{OH} = \text{HOCH}_2\text{O}$

3.5 Impact of update on H abstraction reactions based on new data

We have shown that the H abstraction routes by OH in the investigated n -butanol mechanism, especially those from the α and γ carbon sites, are important for accurate prediction of ignition delay times in the RCM and species concentrations in the JSR. A recent study by McGillen [41] provided updated site specific rate constants for each site, albeit based on measurements

at lower temperatures than of interest here. As a final sensitivity test we therefore updated the four H abstraction rate constants by OH based on the new rate data from [41]. Figure 1 showed the results obtained with the updated mechanism in comparison with predictions from the original mechanism and Weber data [23] for $\phi = 0.5-2$ and $P = 15-30$ bar. The update led to a decrease in the predicted ignition delay times across all conditions studied and therefore better agreement with the measured data under lean conditions at higher temperatures and 15 bar. This is consistent with the findings in [42] where the same updates to the Sarathy mechanism led to significant improvement in the reactivity of *n*-butanol at lower temperatures. While there is also significant improvement in the predicted reactivity under stoichiometric conditions, particularly at $P = 30$ bar (Fig. 2), the agreement with the measured data is worsened at lower pressures (i.e. $P = 15$ bar) under stoichiometric conditions (Fig. 2).

4.0 Discussion and conclusions

A global uncertainty and sensitivity study of the low-intermediate temperature oxidation of *n*-butanol has been conducted within the context of ignition delay times prediction in an RCM and species concentration modelling in a JSR. The study incorporates the effects of uncertainties in the rate constants of the adopted mechanisms on the predicted target outputs, based on a global approach, in order to quantify errors bars which provide information on the robustness of the mechanism over a range of operating conditions. In some cases the uncertainties for predicted target properties of log (ignition delays) and species concentrations spanned over an order of magnitude. A variance-based global sensitivity analysis was carried out to identify and rank the rate parameters driving these predicted uncertainties.

Some key differences in reaction importance were noted when comparing the results of the global sampling based sensitivity analysis when compared to the local linear sensitivity analysis presented in Figs. 5 and 6 for the RCM and JSR respectively. For example, in the local analyses $\text{H}_2\text{O}_2 + \text{M}$ is often the highest ranked reaction. However, due to its low uncertainty, it contributes very little to the overall output variance for any of the targets and would not therefore be a reaction that was targeted for better quantification. Conversely, the reaction $\text{CH}_2\text{O} + \text{OH}$ has two product channels. In the global analysis the formation of HOCH_2O is ranked very highly but is not ranked within the top reactions in the local analysis where the $\text{HCO} + \text{H}_2\text{O}$ channel dominates. These differences arise because more the commonly used local sensitivity analyses do not account for the level of uncertainty present for the input

parameter, or any non-linearities in the response of the target output to changes in the input. Such non-linearity was shown here for the reaction of *n*-butanol + HO₂.

The global sensitivity indices show that in the context of ignition delay prediction, the dominant reaction pathways are H abstraction via OH. The study indicates that low temperature ignition delay measurements provide a high level of constraint on the branching ratio for abstraction by OH from the α and γ sites but not on the total rate constant. For rich conditions R + O₂ and subsequent pathways are equally as important as H abstraction. In the HDMR analysis of the predicted *n*-C₄H₉OH and CH₂O concentration profiles in the JSR at low temperatures (800 K), about 55-70% of the overall predicted uncertainties are accounted for by about 10 reactions as compared to 7 which accounted for over 85% of the predicted uncertainties in the case of the RCM. Also, H abstraction reaction by HO₂ (*n*-C₄H₉OH + HO₂ = C₄H₈OH-1 + H₂O₂) dominated the predicted *n*-butanol and formaldehyde uncertainties in contrast to H abstraction reaction by OH which was more important in the case of the RCM. A reasonable contribution to predicted variance also comes from H abstraction via OH from the γ and α sites with the α site dominating predicted *n*-C₄H₉OH profiles at higher temperatures. In general, better constraint is provided on the *n*-C₄H₉OH + HO₂ abstraction rate by the measured species profiles of *n*-C₄H₉OH and CH₂O at lower temperatures. Current uncertainties in the rate of C₄H₉OH + HO₂ system, suggest the need for detailed and more accurate studies of this reaction rate across a wide range of temperatures and pressures in order to bring predicted targets in better agreement with experimental data.

Acknowledgements

This article is based upon work from COST Action SMARTCATs (CM 1404), supported by COST (European Cooperation in Science and Technology www.cost.eu). We also thank the Tertiary Education Trust Fund (TETFUND), Nigeria, for scholarship funding for E. Agbro.

References

1. Battin-Leclerc, F., E. Blurock, R. Bounaceur, R. Fournet, P.-A. Glaude, O. Herbinet, B. Sirjean and V. Warth. Towards cleaner combustion engines through groundbreaking detailed chemical kinetic models. *Chemical Society Reviews*, 2011, **40**(9), pp.4762-4782.
2. Gopal, M.G. and D.S. Rajendra. Experimental Study on SI Engine At Different Ignition Timing Using CNG And Gasoline-20% n Butanol Blend. *International Journal of Emerging Technology and Advanced Engineering*, 2013, **3**(3), pp.249-255.

3. Srinivasan, A.C. and C.G. Saravanan. Study of Combustion Characteristics of an SI Engine Fuelled with Ethanol and Oxygenated Fuel Additives. *Journal of Sustainable Energy & Environment*, 2013, **1**(2), pp.85-91.
4. Sarkar, A., A. Datta and B.K. Mandal. Performance characteristics of spark ignition engine using ethanol as fuel at different operating conditions. *International Journal of Emerging Technology and Advanced Engineering*, 2013, **3**, pp.96-100.
5. Wigg, B., R. Coverdill, C.-F. Lee and D. Kyritsis. Emissions Characteristics of Neat Butanol Fuel Using a Port Fuel-Injected, Spark-Ignition Engine. *In. SAE International*, 2011.
6. Skevis, G. Liquid Biofuels: Biodiesel and Bioalcohols. *In: F.W. Maximilian Lackner, And Avinash K. Agarwal, ed. Handbook of Combustion*. Weinheim: WILEY-VCH 2010, p.366.
7. Baulch, D.L. Kinetic Databases. *In: M.J. Pilling, ed. Comprehensive Chemical Kinetics: Low Temperature Combustion and Auto-ignition*. Elsevier, 1997.
8. Komninos, N.P. and C.D. Rakopoulos. Modeling HCCI combustion of biofuels: A review. *Renewable and Sustainable Energy Reviews*, 2012, **16**(3), pp.1588-1610.
9. Vancoillie, J. and S. Verhelst. Modeling the combustion of light alcohols in SI engines: a preliminary study. *In: Proceedings of the FISITA 2010 World Automotive Congress*, 2010, pp.1-12.
10. Perini, F. *Optimally reduced reaction mechanisms for Internal Combustion Engines running on biofuels*. PhD thesis, Università di Modena e Reggio Emilia, 2011.
11. Sarathy, S.M., P. Oßwald, N. Hansen and K. Kohse-Höinghaus. Alcohol combustion chemistry. *Progress in Energy and Combustion Science*, 2014, **44**, pp.40-102.
12. Sarathy, S.M., S. Vranckx, K. Yasunaga, M. Mehl, P. Oßwald, W.K. Metcalfe, C.K. Westbrook, W.J. Pitz, K. Kohse-Höinghaus and R.X. Fernandes. A comprehensive chemical kinetic combustion model for the four butanol isomers. *Combustion and Flame*, 2012, **159**(6), pp.2028-2055.
13. Yang, B., P. Oßwald, Y. Li, J. Wang, L. Wei, Z. Tian, F. Qi and K. Kohse-Höinghaus. Identification of combustion intermediates in isomeric fuel-rich premixed butanol–oxygen flames at low pressure. *Combustion and Flame*, 2007, **148**(4), pp.198-209.
14. Dagaut, P., S.M. Sarathy and M.J. Thomson. A chemical kinetic study of n-butanol oxidation at elevated pressure in a jet stirred reactor. *Proceedings of the Combustion Institute*, 2009, **32**(1), pp.229-237.
15. Sarathy, S., M. Thomson, C. Togbé, P. Dagaut, F. Halter and C. Mounaim-Rousselle. An experimental and kinetic modeling study of n-butanol combustion. *Combustion and Flame*, 2009, **156**(4), pp.852-864.
16. Black, G., H.J. Curran, S. Pichon, J.M. Simmie and V. Zhukov. Bio-butanol: Combustion properties and detailed chemical kinetic model. *Combustion and Flame*, 2010, **157**(2), pp.363-373.
17. Moss, J.T., A.M. Berkowitz, M.A. Oehlschlaeger, J. Biet, V. Warth, P.-A. Glaude and F. Battin-Leclerc. An experimental and kinetic modeling study of the oxidation of the four isomers of butanol. *The Journal of Physical Chemistry A*, 2008, **112**(43), pp.10843-10855.
18. Grana, R., A. Frassoldati, T. Faravelli, U. Niemann, E. Ranzi, R. Seiser, R. Cattolica and K. Seshadri. An experimental and kinetic modeling study of combustion of isomers of butanol. *Combustion and Flame*, 2010, **157**(11), pp.2137-2154.
19. Harper, M.R., K.M. Van Geem, S.P. Pyl, G.B. Marin and W.H. Green. Comprehensive reaction mechanism for n-butanol pyrolysis and combustion. *Combustion and Flame*, 2011, **158**(1), pp.16-41.
20. Zhou, D.D.Y., M.J. Davis and R.T. Skodje. Multitarget Global Sensitivity Analysis of n-Butanol Combustion. *The Journal of Physical Chemistry A*, 2013, **117**(17), pp.3569-3584.
21. Weber, B.W. and C.-J. Sung. Comparative Autoignition Trends in Butanol Isomers at Elevated Pressure. *Energy & Fuels*, 2013, **27**(3), pp.1688-1698.

22. Goodwin, D.M., N; Moffat, H; Speth, R. *CANTERA: an object-oriented software toolit for chemical kinetics, thermodynamics, and transport processes*. 2.0.2 ed. <https://code.google.com/p/cantera>, 2013.
23. Weber, B.W., K. Kumar, Y. Zhang and C.-J. Sung. Autoignition of n-butanol at elevated pressure and low-to-intermediate temperature. *Combustion and Flame*, 2011, **158**(5), pp.809-819.
24. Mittal, G. and C.-J. Sung. A rapid compression machine for chemical kinetics studies at elevated pressures and temperatures. *Combustion Science and Technology*, 2007, **179**(3), pp.497-530.
25. Weber, B.W. *GitHub account* (<https://github.com/bryanwweber/CanSen>). [Accessed July 2014].
26. Sung, C.J. *Experimental Database; available at <http://combdialab.engr.uconn.edu/database>*. [Accessed May 2014]. 2014.
27. Baulch, D.L., C.T. Bowman, C.J. Cobos, R.A. Cox, T.H. Just, J.A. Kerr, M.J. Pilling, D. Stocker, J. Troe, W. Tsang, R.W. Walker and J. Warnatz. Evaluated kinetic data for combustion modeling: supplement II. *Journal of Physical and Chemical Reference Data*, 2005, **34**, pp.757-1397.
28. Baulch, D.L., C.J. Cobos, R.A. Cox, J.H. Frank, G. Hayman, T.H. Just, J.A. Kerr, T. Murrels, Pilling, J. M. J.; Troe, B.F. Walker and J. Warnatz. Summary table of evaluated kinetic data for combustion modeling: Supplement 1. *Combustion and Flame*, 1994, pp.59-79.
29. Baulch, D.L., C.J. Cobos, R.A. Cox, C. Esser, P. Frank, T. Just, J.A. Kerr, M.J. Pilling, J. Troe, R.W. Walker and J. Warnatz. Evaluated Kinetic Data for Combustion Modelling. *Journal of Physical and Chemical Reference Data*, 1992, **21**(3), pp.411-734.
30. Tsang, W. Chemical Kinetic Data Base for Propellant Combustion. II. Reactions Involving CN, NCO, and HNCO. *Journal of Physical and Chemical Reference Data*, 1992, **21**(4), pp.753-791.
31. Tsang, W. and R.F. Hampson. Chemical Kinetic Data Base for Combustion Chemistry. Part I. Methane and Related Compounds. *Journal of Physical and Chemical Reference Data*, 1986, **15**(3), pp.1087-1279.
32. Tomlin, A.S. and T. Turanyi. Investigation and Improvement of Mechanism using Sensitivity Analysis and Optimization. In: F. Battin-Leclerc, J.M. Simmie and E. Blurock, eds. *Cleaner Combustion: Developing Detailed Chemical Kinetic Models* London: Springer-Verlag, 2013.
33. Tomlin, A.S. The role of sensitivity and uncertainty analysis in combustion modelling. *Proceedings of the Combustion Institute*, 2013, **34**(1), pp.159-176.
34. Tomlin, A.S., E. Agbro, V. Nevrlý, J. Dlabka and M. Vašinek. Evaluation of Combustion Mechanisms Using Global Uncertainty and Sensitivity Analyses: A Case Study for Low-Temperature Dimethyl Ether Oxidation. *International Journal of Chemical Kinetics*, 2014, **46**(11), pp.662-682.
35. Heufer, K., R. Fernandes, H. Olivier, J. Beeckmann, O. Röhl and N. Peters. Shock tube investigations of ignition delays of n-butanol at elevated pressures between 770 and 1250K. *Proceedings of the Combustion Institute*, 2011, **33**(1), pp.359-366.
36. Da Silva, G., J.W. Bozzelli, L. Liang and J.T. Farrell. Ethanol oxidation: Kinetics of the α -hydroxyethyl radical+ O₂ reaction. *The Journal of Physical Chemistry A*, 2009, **113**(31), pp.8923-8933.
37. Westbrook, C.K., M. Mehl, W.J. Pitz and M. Sjöberg. Chemical kinetics of octane sensitivity in a spark-ignition engine. *Combustion and Flame*, 2017, **175**, pp.2-15.
38. Zhou, C.-W., J.M. Simmie and H.J. Curran. Rate constants for hydrogen-abstraction by from n-butanol. *Combustion and Flame*, 2011, **158**(4), pp.726-731.
39. Zador, J. and J.A. Miller. *Hydrogen Abstracyion from ni--Propanol and n-Butanol: A Systematic Theorecal Approach*. Sandia National Laboratories (SNL-CA), Livermore, CA (United States), 2011.

40. Pang, G.A., R.K. Hanson, D.M. Golden and C.T. Bowman. Rate Constant Measurements for the Overall Reaction of OH + 1-Butanol \rightarrow Products from 900 to 1200 K. *The Journal of Physical Chemistry A*, 2012, **116**(10), pp.2475-2483.
41. McGillen, M.R., M. Baasandorj and J.B. Burkholder. Gas-Phase Rate Coefficients for the OH + n-, i-, s-, and t-Butanol Reactions Measured Between 220 and 380 K: Non-Arrhenius Behavior and Site-Specific Reactivity. *The Journal of Physical Chemistry A*, 2013, **117**(22), pp.4636-4656.
42. Agbro, E., A.S. Tomlin, M. Lawes, S. Park and S.M. Sarathy. The influence of n-butanol blending on the ignition delay times of gasoline and its surrogate at high pressures. *Fuel*, 2017, **187**, pp.211-219.